

In vitro and in vivo evaluation of β -cyclodextrin-based nanosponges of telmisartan

Monica Rao · Amrita Bajaj · Ishwar Khole · Ghanshyam Munjapara · Francesco Trotta

Received: 8 August 2011 / Accepted: 19 July 2012 / Published online: 23 August 2012
© Springer Science+Business Media B.V. 2012

Abstract Telmisartan (TEL) is a BCS Class II drug having dissolution rate limited bioavailability. The aim of work was to enhance the solubility of TEL so that bioavailability problems are solved. β -Cyclodextrin (β -CD) based nanosponges (NSs) were formed by cross-linking β -CD with carbonate bonds, which were porous as well as nanosized. Drug was incorporated by solvent evaporation method. The effect of ternary component alkalizer (NaHCO_3) on solubility of TEL was studied. In order to find out the solubilization efficiency of NS, phase solubility study was carried out. Saturation solubility and in vitro dissolution study of β -CD complex of TEL was compared with plain TEL and NS complexes of TEL. The NS and NS complexes of TEL were characterized by differential scanning calorimetry, powder X-ray diffraction, Fourier transform infrared spectroscopy, nuclear magnetic resonance and scanning electron microscope. It was found that solubility of TEL was increased by 8.53-fold in distilled water; 3.35-fold in 0.1 N HCl and 4.66-fold in phosphate buffer pH 6.8 by incorporating NaHCO_3 in drug–NS complex than TEL. It was found that the NaHCO_3 in NS based complex synergistically enhanced dissolution of TEL by modulating microenvironmental pH and by

changing amorphization of the drug. The highest solubility and in vitro drug release was observed in inclusion complex prepared from NS and NaHCO_3 . An increase of 54.4 % in AUC was seen in case the ternary NS complex whereas β -CD ternary complex exhibited an increase of 79.65 %.

Keywords Nanosponge · Telmisartan · β -Cyclodextrin · Sodium bicarbonate

Introduction

Polymers used in drug delivery systems are naturally occurring polysaccharides, which always appear as attractive alternative due to low cost, high biodegradability and biocompatibility [1]. Amongst all of the cyclodextrins (CDs), β -CDs have been the most widely used cyclic oligomer [2–4].

β -CD are the building-blocks for nanosponge (NS). They are linked by carbonyl group of cross-linker to form a highly cross-linked network. The reaction is carried out under relative mild conditions. The final NS structure forms a network of more hydrophilic channels which contains both CD lipophilic cavities and carbonate bridges (Fig. 1) [5]. Structural characterization of NS showed that the carbonyl group of cross-linker get connected to the primary hydroxyl groups of the parent β -CD unit (Fig. 1). There was formation of nanochannels in the NS structure due to cross-linking network thus creating potential spaces/cavities for drug molecules to be entrapped not only in the nanocavities of β -CD but also within the nanochannels in the NS. In comparison with the parent CD, peculiar structural organization of NS might be responsible for the increased solubilization and protection capacities [6].

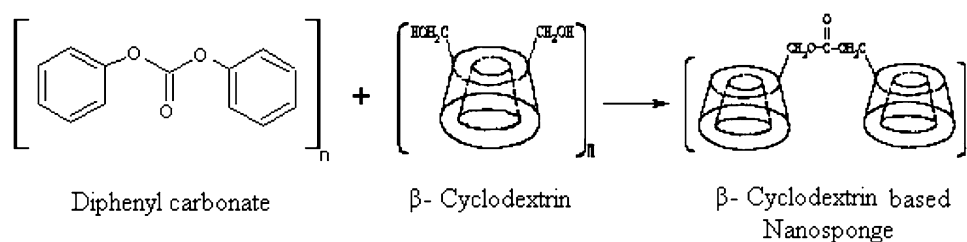
Telmisartan (TEL) is an antihypertensive drug, which is angiotensin II receptors (AT1) antagonist. Due to the

M. Rao (✉) · I. Khole · G. Munjapara
Department of Pharmaceutics, AISSMS College of Pharmacy,
Near RTO, Kennedy Road, Pune 411 001, Maharashtra, India
e-mail: monicarp_6@hotmail.com

A. Bajaj
Head of Department (Pharmaceutics), SVKM's B. N. College
of Pharmacy, Mumbai, Maharashtra, India

F. Trotta
Department of Chemistry IFM, University of Torino, Torino,
TO, Italy

Fig. 1 Schematic representation of chemical reaction for formation of NS



minimal side effects of drug, therapy with this drug offers a good quality of life for hypertensive patients [7]. According to the chemical structure of TEL, it is readily ionizable and the solubility is also pH dependent. Physicochemically it can be characterized as very poorly water soluble drug, resulting in low bioavailability [8]. The aqueous solubility of the compound is estimated to be 9.9 $\mu\text{g/ml}$ at neutral pH [9].

The objective of the work was to investigate and compare the role of β -CD and NS of β -CD to enhance the solubility and dissolution rate of TEL by preparing binary and ternary inclusion complexes and to conduct pharmacokinetic studies on some of the complexes to corroborate in vitro results.

Materials and methods

TEL was obtained as a sample from Unichem Laboratories India. β -CD was purchased from S. D. Fine Chemicals Ltd., Mumbai [India]. Diphenyl carbonate (DPC) was purchased from Spectrochem Pvt. Ltd. Mumbai [India]. All other reagents and solvents were of analytical grade.

Synthesis of β -CD NS

β -CD based NS was prepared using DPC as a cross-linker [10]. NSs were prepared using different ratios of β -CD and DPC [1:2, 1:4 and 1:6]. The schematic representation of chemical reaction for the formation of NS is depicted in Fig. 1. Finely homogenized anhydrous β -CD and DPC were placed in a 250 ml conical flask. The system was gradually heated to 100 $^{\circ}\text{C}$ under magnetic stirring, and left to react for 5 h. During the reaction crystals of phenol appeared at the neck of the flask. The reaction mixture was left to cool and product obtained was broken up roughly. The solid was repeatedly washed with distilled water to remove unreacted β -CD and then with acetone, to remove the unreacted DPC and the phenol present as by-product of the reaction. After purification, NSs were stored at 25 $^{\circ}\text{C}$ until further use.

Phase solubility studies

Phase solubility equilibrium plots were obtained for binary system at 25 $^{\circ}\text{C}$ in distilled water. The studies were

performed according to the method reported by Higuchi and Connors [11]. Studies for binary systems of drug- β -CD and drug-NS were carried out by adding excess amount of drug to the 20 ml of aqueous solution containing increasing concentration of β -CD/NS. The contents were stirred for 48 h at 25 ± 0.5 $^{\circ}\text{C}$. After equilibrium, the samples were filtered and absorbance read at 296 nm (Jasco UV/Vis spectrophotometer).

Solution state interaction studies [12]

Increasing concentrations of NS solutions (1–80 ppm) were added to fixed concentrations of TEL (10 ppm). The samples were then kept overnight for interaction and scanned for λ_{max} and absorbances were measured. The parameter studied was spectral shift.

Molecular modeling studies

Schrodinger 2008 software was used to carry out molecular modeling studies akin to docking studies routinely carried out by synthetic chemists. The three dimensional structures of TEL, β -CD and NS were drawn using the software and attempt was made to deduce the possible mode of entrapment of TEL into NS and β -CD structure.

Preparation of TEL-loaded NS

TEL was dissolved in dichloromethane to form a solution. To this solution NS and sodium bicarbonate were added and triturated until the solvent evaporated. The NaHCO_3 , TEL and NS, were added in a ratio of 1:8:16 by weight. The solid dispersion was dried in an oven overnight (at 50 $^{\circ}\text{C}$ at atmospheric pressure) to remove any traces of dichloromethane and sieved through 60 # and used for further work. Similar procedure was used to prepare TEL loaded NS (1:2) and β -CD complex of TEL (1:2) with and without NaHCO_3 (Table 1).

Evaluation of NS and complexes

NSs with three different β -CD-DPC ratios were prepared. Preliminary dissolution trials for studying the effect of inclusion complexation of TEL with the various NSs

Table 1 Coding for different inclusion complexes

Sr. no.	Inclusion complexes	Code
1.	Inclusion complex of NS1 and TEL	IC1
2.	Inclusion complex of NS2 and TEL	IC2
3.	Inclusion complex of NS3 and TEL	IC3
4.	Inclusion complex of β -CD and TEL	IC4
5.	NaHCO ₃ containing inclusion complexes of NS1 and TEL	IC5
6.	NaHCO ₃ containing inclusion complexes of NS2 and TEL	IC6
7.	NaHCO ₃ containing inclusion complexes of NS3 and TEL	IC7
8.	NaHCO ₃ containing inclusion complexes of β -CD and TEL	IC8

revealed that at 1:2 ratio, the degree of cross-linking may be low and hence insufficient nanochannels are created which do not have a significant impact of the dissolution of TEL. At 1:6 ratios the degree of cross-linking may be too high so that more complex and tortuous nanochannels are created which prevent the entrapment of TEL into the NS structure. The NSs synthesized using 1:4 β -CD-crosslinker ratio (NS2) was found to have a desirable impact on the dissolution profile. Hence further studies were conducted using these NSs.

Saturation solubility studies

Excess drug/binary or ternary complexes were added to 20 ml of distilled water, 0.1 N HCl, phosphate buffer pH 6.8, fasting state simulated intestinal fluid (FaSSIF) and fed state simulated intestinal fluid (FeSSIF) separately and were equilibrated on a mechanical shaker at 25 ± 0.5 °C for 24 h. The equilibrated suspensions were filtered through membrane filter (0.45 μ m) and assayed for drug content by developed HPLC method. The studies were performed in triplicate. FaSSIF and FeSSIF were prepared as per formula and procedure described by Marques [13].

HPLC analysis of TEL

The concentration of TEL was determined by RP-HPLC (Agilent Technologies 1120 series, Germany) using TC-C18 column (4.6 \times 250 mm, 5 μ m). Acetonitrile and 0.05 M potassium dihydrogen phosphate in a ratio 60:40 (adjusted to pH 3.0 with o-phosphoric acid) was used as the mobile phase at a flow rate of 1 ml/min. The eluent was analyzed at 271 nm by UV detector. The method was validated for accuracy, precision and recovery.

Porosity

Porosity of β -CD and NS were found out by using Helium Pycnometer (HP-2000, S. P. Consultant Mumbai). Helium gas has the ability to penetrate inter- and intra-particular

spaces of material. True volume of material was determined by helium displacement method and % porosity calculated by following formula.

$$\% \text{ Porosity} = \frac{\text{bulk volume} - \text{true volume}}{\text{bulk volume}} \times 100 \quad (1)$$

Fourier transform infrared spectroscopy (FTIR)

IR spectra was recorded using a Jasco FTIR—460 Plus spectrophotometer in order to find out the interaction between TEL and NS as well as to confirm the formation of NS. About 1–2 mg of sample was mixed with 50 mg dry potassium bromide and the samples were examined in transmission mode over wave number range of 4,000–400 cm^{-1} .

Differential scanning calorimetry (DSC)

Thermograms were obtained using a METTLER TOLEDO DSC823° differential scanning calorimeter. A heating rate 10 °C/min were employed in the 30–300 °C temperature range. Standard aluminum sample pans were used; an empty pan was used as reference standard. Analyses were performed on 5 mg samples under nitrogen purge (40 ml/min).

Powder X-ray diffraction (PXRD)

The PXRD spectra of samples were recorded using high power powder X-ray diffractometer (Ru-200B) with Cu as target filter having a voltage/current of 40 kV/40 mA at a scan speed of 4°/min. The samples were analyzed at 2 θ angle range of 5°–50°. Step time was 0.5 s and time of acquisition was 1 h.

¹³C nuclear magnetic resonance (NMR)

¹³C NMR spectra of NS and β -CD were taken by using Verian-NMR-mercury 300 spectrometer. The stock solutions of NS and β -CD were prepared in deuterated-DMSO.

Particle size analysis and zeta potential

The NSs were dispersed in distilled water and sonicated in a bath sonicator for 20 min. The dispersion obtained was then diluted suitably with distilled water and particle size was measured using Delsa™ Nano Beckmann coulter. Zeta potential was measured in same instrument, by placing plain NS in the flow cell. Average electric field of about 16.25 V/cm and average current of about 0.05 mA was applied.

Scanning electron microscopy (SEM)

The surface morphology of samples was determined using analytical scanning electron microscope (JSM-6360A, JEOL, Tokyo, Japan). The samples were lightly sprinkled on a double adhesive tape stuck to an aluminum stub. The stubs were then coated with platinum to a thickness of about 10 Å under an argon atmosphere using a gold sputter module in a high-vacuum evaporator. The stub containing the coated samples was placed in the scanning electron microscope chamber.

In vitro dissolution studies

Dissolution studies on the formulations were performed in triplicate in 900 ml of 0.1 N HCl, distilled water and buffer of pH 6.8 using USP paddle type dissolution apparatus at 37 ± 0.5 °C at 100 rpm. Samples were withdrawn at pre-determined intervals and analyzed by previously mentioned HPLC method.

In vivo studies

Approval to carry out in vivo study was obtained from Institutional Animal Ethics Committee, AISSMS College of Pharmacy (Approval No. AISSMS/IAEC/09-10/02-05) and their guidelines were followed for the studies. The in vivo performance of the complexes and TEL was evaluated in rats (Wistar albino rat). Three groups (standard, test₁ and test₂) of six rats each weighing 150–250 g, were fasted overnight before administration of drug. Formulations for rats were prepared considering the dose of TEL as 4 mg/kg [14]. The suspension of ternary complexes of TEL (IC6 and IC8) and TEL was prepared in water. These suspensions were administered orally to rats through feeding needle to bypass trachea. The rats were anesthetized using ether and the blood samples (1 ml) were withdrawn from the retro orbital vein at 0 (pre-dose), 0.5, 2, 4, 6, and 8 h in vacutainer tubes containing anti-coagulant, mixed and centrifuged at 3,000 rpm for 30 min. The plasma was separated carefully and stored at 2–10 °C until drug analysis was carried. HPTLC method was developed to find out

the concentration of drug in plasma. Methanol was added to plasma in the ratio of 3:1 as a precipitating agent. Samples were vortexed and then centrifuged at 10,000 rpm for 10 min at 4 °C. The concentration of the TEL was calculated using the calibration curve prepared in plasma.

HPTLC analysis

The samples were spotted on Merck TLC aluminium plates, precoated with silica gel 60F 254 (10 cm × 20 cm with 250 µm layer thickness) using a Camag Linomat V applicator (Camag, Switzerland). The samples were applied onto the TLC plates in the form of narrow bands of 6 mm width with a Camag 100 µl sample syringe under a nitrogen atmosphere. The TLC plates were developed in solvent system of toluene–methanol (8:2). The length of the chromatographic run was set to 8 cm. Linear ascending development was carried out in a twin trough glass chamber (10 cm × 20 cm). Densitometric scanning of the developed plates was performed using Camag TLC scanner III, in the absorbance mode at 296 nm. Scanning speed was kept at 4 mm/s. The concentration of TEL in each sample was calculated using the areas obtained by densitometric scanning. From the plot of plasma concentration versus time, area under curve at the end of 8 h ($AUC_{8\text{ h}}$), C_{max} (maximum concentration) and t_{max} (time for C_{max}) were calculated using the trapezoidal rule [15].

Results and discussion

Phase solubility studies

The phase solubility diagram for the TEL-NS system in water is depicted in the Fig. 2. A linear increase in the solubility of TEL was observed with increasing concentration of NS. The phase solubility plot showed an A_L curve for NS which indicated formation of inclusion complex of NS with TEL in 1:2 stoichiometric ratio. The

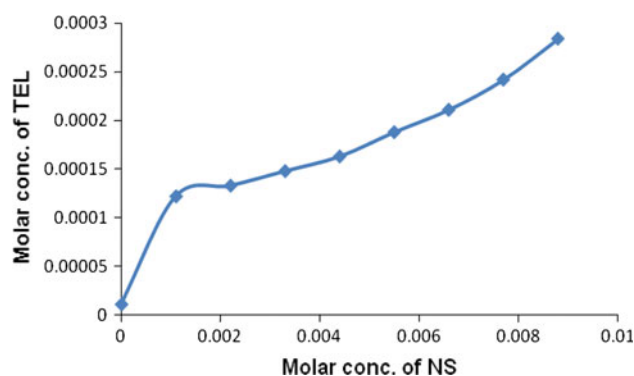


Fig. 2 Phase solubility diagram in water

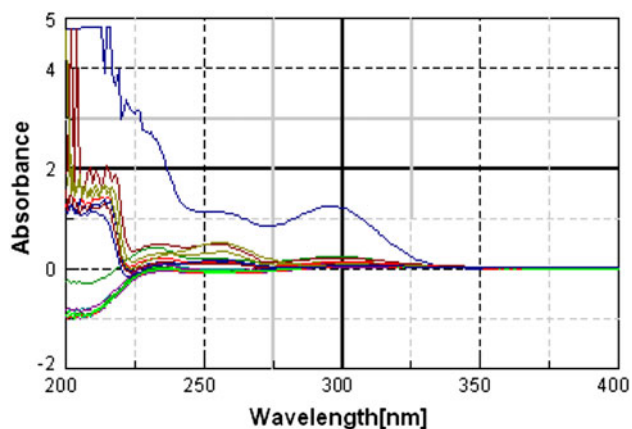


Fig. 3 Solution state interaction studies spectra of TEL in presence of increasing concentration of nanosponge

stability constant for complex at 25 °C, assuming a 1:2 stoichiometry, calculated from the linear portion of phase solubility curve was found to be 255.102 M^{-1} for TEL:NS which indicated stable complex formation. Stability constant should be between 150 and $2,000 \text{ M}^{-1}$ which indicates good complexation ability. The stability constant for the inclusion complex of TEL with β -CD was found to be 428.52 M^{-1} thus alluding to greater affinity and more stable complex formation between TEL and β -CD.

Solution state interaction studies

The drug was found to absorb ultraviolet light at 296 nm (Fig. 3). As the concentration of NS increased, the shift in the

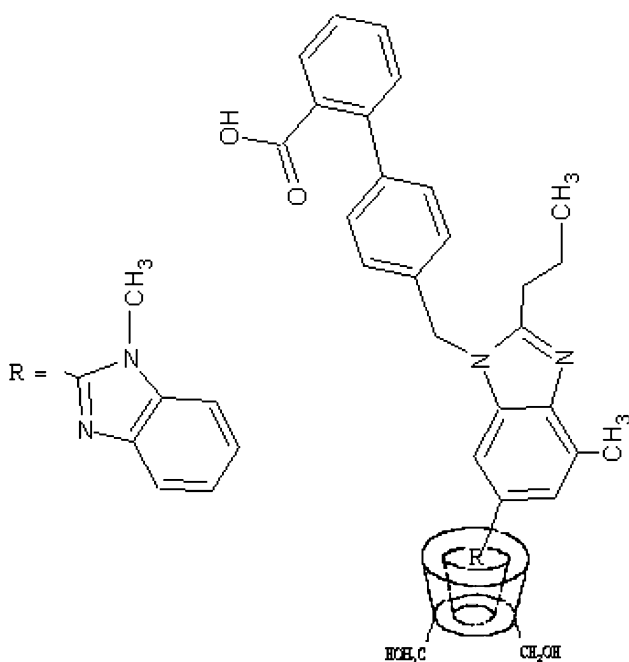


Fig. 4 Inclusion complex of β -CD and TEL

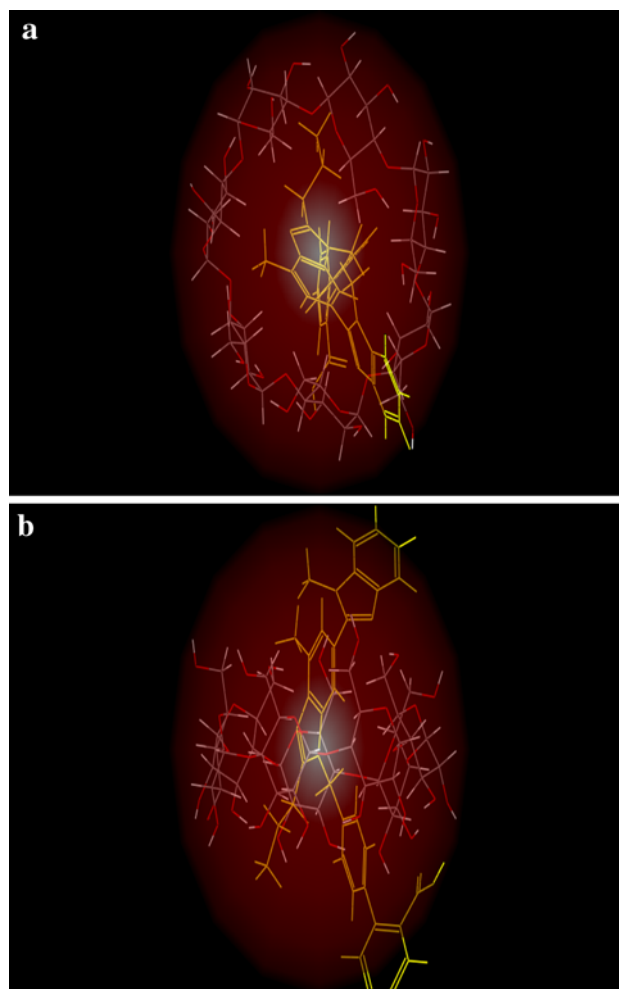


Fig. 5 3D image showing possible mode of entrapment of TEL in **a** β -CD, **b** NS

wavelength also increased. The peak of plain drug was masked at 10 ppm of NS concentration. Modification of UV-spectra in presence of CDs/NSs provides evidence of formation of inclusion complex. As CD concentration increases the spectra show a shift of the maximum absorption to lower wavelengths and a decrease in molar extinction coefficients. This suggests that the chromophore of the guest is transferred from an aqueous medium to the non polar CD cavity. These changes must be due to a perturbation of electronic energy levels of guest molecule either by direct interaction with CD, by exclusion of solvating water molecules or by combination of these two effects [16].

Evaluation of NS and complexes

Saturation solubility studies

TEL molecule consists of three major functional groups i.e. methylbenzimidazol, propylbenzimidazol and methylphenyl benzoic acid. Investigation of the different functional

Table 2 Saturation solubility studies of TEL in distilled water

Type	Solubility ($\mu\text{g/ml} \pm \text{RSD}$)	Enhancement factor
TEL	9.9 ± 0.89	–
IC2	45.92 ± 0.55	4.63
IC4	57.22 ± 1.21	5.77
IC6	84.46 ± 0.98	8.53
IC8	203.4 ± 0.65	20.54

 $n = 3$ **Table 3** Saturation solubility studies of TEL in 0.1 N HCl and phosphate buffer pH 6.8

Type	Solubility ($\mu\text{g/ml} \pm \text{RSD}$)	Enhancement factor
0.1 N HCl		
TEL	36.47 ± 0.58	–
IC2	78.3 ± 1.57	2.14
IC4	92.5 ± 1.5	2.53
IC6	122.4 ± 1.32	3.35
IC8	150.1 ± 1.09	4.11
Phosphate buffer pH 6.8		
TEL	14 ± 0.72	–
IC2	52.12 ± 1.21	3.72
IC4	75.12 ± 0.86	5.36
IC6	65.25 ± 1.45	4.66
IC8	266.6 ± 0.57	19.04

 $n = 3$ **Table 4** Saturation solubility studies of TEL in FaSSIF and FeSSIF

Type	Solubility ($\mu\text{g/ml} \pm \text{RSD}$)	Enhancement factor
FaSSIF		
TEL	78.84 ± 0.72	–
IC2	150.76 ± 1.57	1.91
IC4	185.23 ± 1.5	2.34
IC6	264.36 ± 1.32	3.35
IC8	521.15 ± 1.09	6.61
FeSSIF		
TEL	38.24 ± 0.58	–
IC2	40.15 ± 1.21	1.05
IC4	42.95 ± 0.86	1.12
IC6	121.35 ± 1.45	3.17
IC8	305.71 ± 0.57	7.99

 $n = 3$

groups of the TEL using Schrödinger 2008 software revealed that the methylbenzimidazol group had a dimension of approximately 6.8 Å. The propylbenzimidazol measured around approximately 11 Å and methylphenyl benzoic acid

Table 5 Percent porosity of β -CD and NSs

Type	β -CD	NS2
True density	0.53	0.55
True volume	5.647	5.419
Bulk volume	6.9	7.8
% Porosity	18.16	30.53

measured approximately 8.4 Å. The first two groups (methylbenzimidazol, propylbenzimidazol) are lipophilic in nature, whereas the last group (methylphenyl benzoic acid) is hydrophilic due to carboxylic acid. β -CD has an internal diameter of 6–6.5 Å and height of the torus is approximately 7.9 Å. From this observation we can say that methylbenzimidazole group is entrapped within β -CD cavity (Fig. 4). The possible mode of entrapment of TEL into the three dimensional structure of β -CD and NS were deciphered using the software (Fig. 5a, b) and it was inferred that TEL may form inclusion complex with β -CD more easily than with NS. This could be possibly due to the tortuous nature of the cavities in the NS. The results of saturation solubility also appeared to support these findings. Saturation solubility of TEL in the β -CD complex was found to be 57.22 $\mu\text{g/ml}$ whereas in NS it was 45.92 $\mu\text{g/ml}$. The reduced saturation solubility of TEL in the NS as compared to β -CD complex may be attributed to the fact that, TEL molecule is not fully getting entrapped in the NS structure due to steric hindrance. However, the solubility of TEL in NS complex was much better than plain TEL.

The solubility of binary systems (NS and drug) and ternary complex (NS, alkalizer and drug) was found to be increased in both D. W., pH 6.8 buffer and 0.1 N HCl (Tables 2, 3, 4). The enhancement factors were also calculated for the same. The solubility was enhanced over 8.53-folds in case of ternary complex and 4.63-folds and 5.77-folds in case of binary complex with NS and β -CD respectively as compared to plain TEL in D.W. Ternary complex with β -CD and NaHCO_3 showed an exponential 20-fold increase in solubility. The solubility was enhanced over 3.35-folds in case of ternary complex and 2.14- and 2.53-folds in case of binary complex with NS and β -CD respectively as compared to plain TEL in 0.1 N HCl. Ternary complex with β -CD and NaHCO_3 exhibited a 4.1-fold enhancement in saturation solubility. Dissociation constant (pK_a) of TEL is 4.45 ± 0.09 . From pH partition hypothesis, it was clear that 99 % of drug was in ionized state in 0.1 N HCl. Therefore, TEL showed high solubility in 0.1 N HCl. The effect of NaHCO_3 in modulating the microenvironmental pH (pH_M) in 0.1 N HCl is not significant as evident from the saturation solubility data. The solubility was enhanced over 4.66-folds in case of ternary

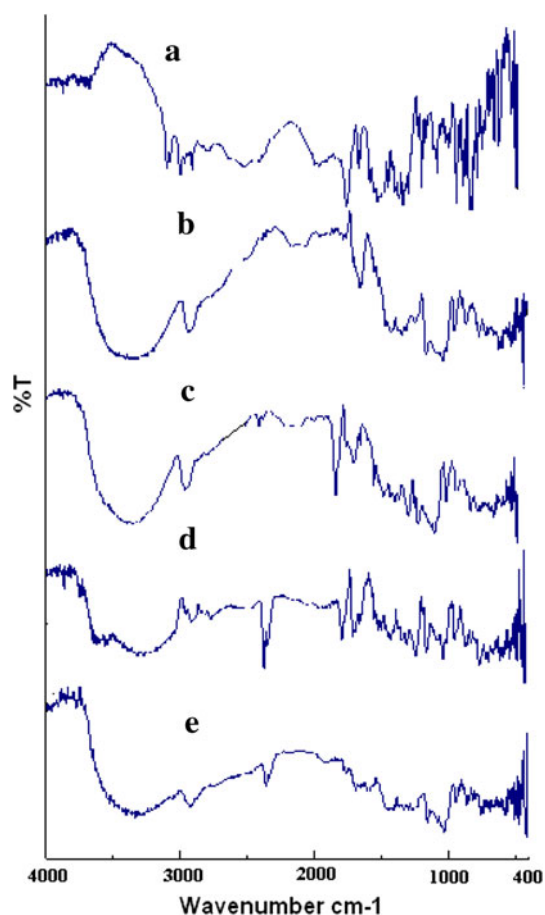


Fig. 6 FTIR spectra of (a) TEL, (b) β-CD, (c) NS, (d) IC2, (e) IC6

complex with NS and 3.72- and 5.36-folds in case of binary complex with NS and β-CD respectively as compared to plain TEL in phosphate buffer pH 6.8 (Table 3). However, β-CD in combination with NaHCO₃ showed an almost 20-fold increase in solubility in phosphate buffer. Peculiar results were observed in biorelevant media i.e. FaSSIF and FeSSIF (Table 4). TEL itself showed higher solubility in biorelevant media. However the binary complex with NS showed a 1.91-fold increase in FaSSIF whereas the ternary complex showed a 3.35-fold increase. Binary complex with β-CD exhibited a 2.34-fold increase and with ternary complex the increase was to the tune of 6.6 times. Interestingly in FeSSIF all the complexes exhibited a marginal increase in saturation solubility in the range of 1.05–3.17 times that of TEL whereas ternary complex with β-CD showed an increase of eightfold. The implications of this would be that though the ternary complex with β-CD showed a remarkable enhancement in solubility of TEL in all media, the NS structure appeared to give a more controlled increase and release profile which may be an important safety consideration. Additionally the release could be modulated (increased/decreased) by inclusion of a third component. In case of TEL, addition of NaHCO₃

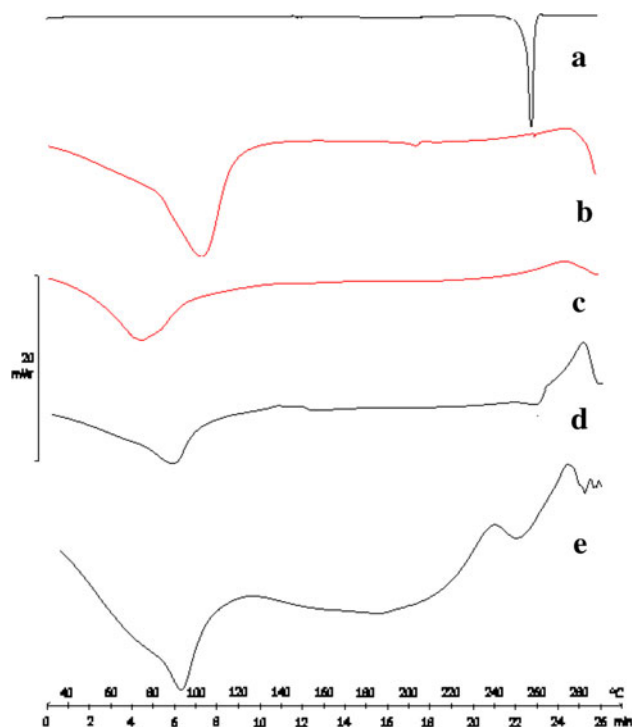


Fig. 7 DSC spectra of (a) TEL, (b) β-CD, (c) NS, (d) IC2, (e) IC6

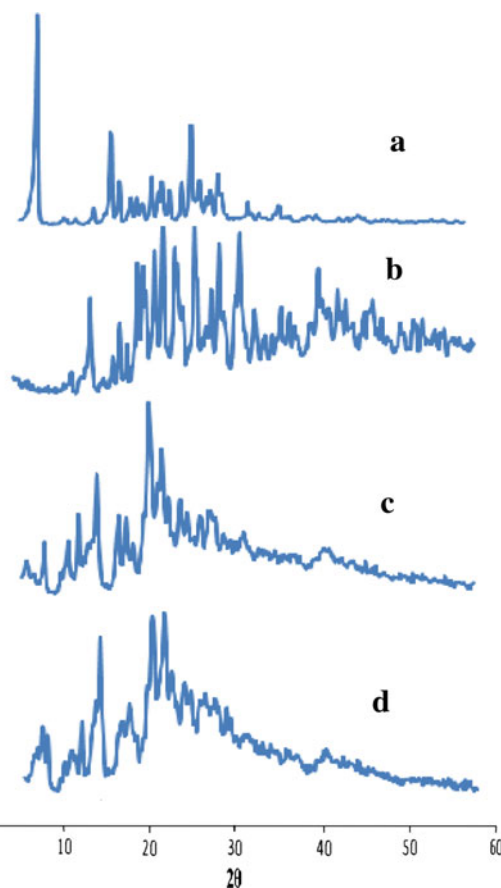
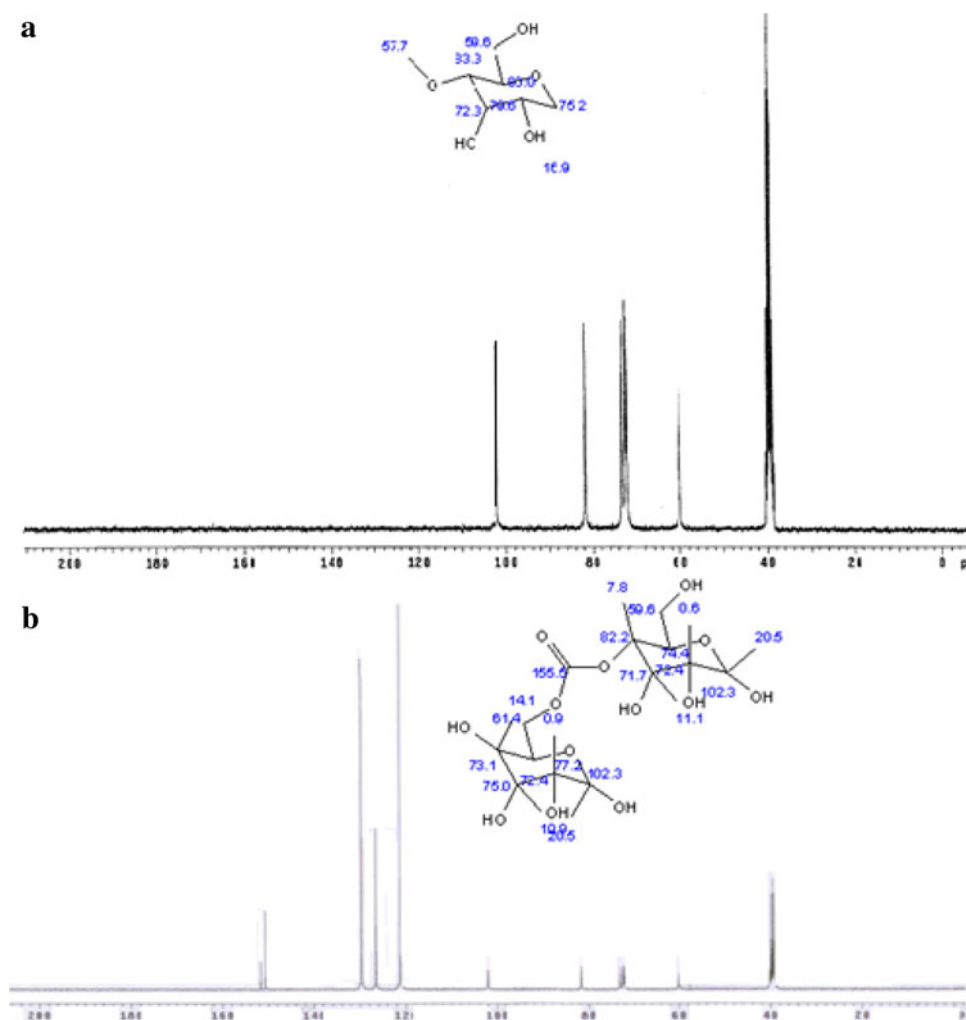


Fig. 8 PXRD pattern of spectra of (a) TEL, (b) β-CD, (c) NS, (d) IC2

Fig. 9 NMR spectra of **a** β -CD, **b** NS



modifies the pH_M to a value conducive for the solubility of TEL. Studies were also conducted with TPGS as the third component, however it did not produce the desired increase in solubility, this despite the fact that TPGS is a surface active agent. Thus it could be attributed to its large molecular size which creates steric hindrance and thereby precludes entrapment of TEL into the NS cavities ultimately affecting its solubility.

Porosity

True volumes of β -CD and NS were obtained by using Helium pycnometer, from which % porosity were calculated by Eq. (1) (Table 5). It was found that 68.12% increase in the porosity of NS as compared to β -CD. Increase in the % porosity of NS can be attributed the presence of the cross-linked network which forms nano-channels in the NS structure. Due to formation of nano-channels, large amount of drug can be incorporated inside

the NS and cross-linking will control the release of drug from NS which was observed in in vitro dissolution profile.

Fourier transform infrared spectroscopy (FTIR)

The characteristic peaks of TEL (Fig. 6a) were at 3673, 1695, 1455, 1381, 1350–1000 cm^{-1} . The FTIR spectra of NS showed a peak at 1,700–1,703 cm^{-1} , which is characteristic of the carbonyl group. It is evident from the profiles reported that the peak at 1,700 cm^{-1} is absent in the FTIR spectrum of β -CD (Fig. 6b, c).

The complexation between TEL and NS was confirmed by FTIR. IR spectra of complex (Fig. 6d) showed broadenings and disappearance of some peaks which might be due to weak interactions between NS and TEL. The drug frequency of the O–H broad band disappeared and the C=O band decreased in the FTIR spectra when $NaHCO_3$ were added (Fig. 6e). It was found that the $NaHCO_3$ in NS based complex synergistically enhanced dissolution of TEL not

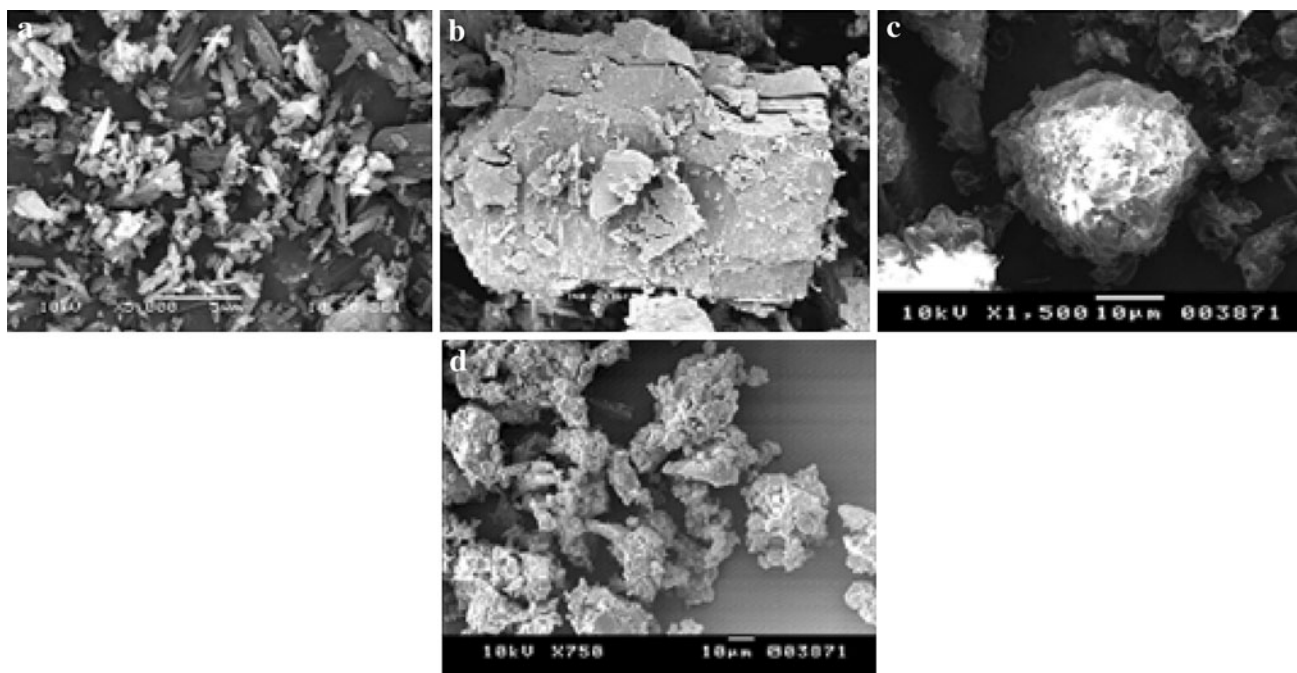


Fig. 10 SEM of **a** TEL, **b** β -CD, **c** NS, **d** IC2

only by modulating pH_M but also by changing drug crystallinity to an amorphous form via molecular interactions.

Differential scanning calorimetry (DSC)

The DSC spectra of TEL (Fig. 7a) showed a sharp endothermic peak at 269 °C corresponding to melting point of TEL. A significant difference between the DSC thermogram of β -CD and NS was evident (Fig. 7b, c). DSC spectra of NS showed absence of peaks before 300 °C indicating stable nature of cross-linked NS.

The complexation between TEL and NS was also confirmed by DSC (Fig. 7d). The thermograms of drug loaded NS did not contain the sharp drug melting peak whereas that of NaHCO_3 added drug loaded NS (Fig. 7e) showed broad and shallow endothermic peak at 260 °C, which might be displaced peak of drug. Thus we can infer that the drug is molecularly dispersed in the NS with the lipophilic portions entrapped within the hydrophobic cavities.

Powder X-ray diffraction (PXRD)

Diffraction pattern of the pure drug TEL shows its highly crystalline nature, indicated by numerous distinctive peaks at a diffraction angle of 2θ [6.8°, 14.2° and 22.3°] throughout the scanning range (Fig. 8a). Formation of NS was confirmed by PXRD spectra. As shown in Fig. 8b and c there was a significant difference between spectra of β -CD and NS i.e. reduction in the numbers and intensity of

peaks. The complex between TEL and NS was also confirmed by PXRD spectra. As shown in the PXRD spectra of drug loaded NS (Fig. 8d), numerous distinctive peaks of TEL gets reduced. Hence, TEL partially incorporated in NS. Thus it can be predicted that the solubility of TEL in case of binary complex is due to masking of hydrophobic groups of TEL by NS.

Nuclear magnetic resonance (NMR)

Figure 9 show that the ^{13}C NMR predicted value of β -CD and NS by using ACD/Chemsketch software. ^{13}C NMR spectra of selected preparations were taken which included β -CD and NS. The presence of peak at 155 ppm in NS spectra (Fig. 9a, b) confirmed the formation of NS from β -CD. By comparing predicted value and spectra, the peak which was found at 155 ppm was of carbonate carbon which links two β -CD molecules.

Particle size and zeta potential analysis

The particle size of the plain NS was found to be 664 nm with a polydispersibility of 0.451. Reduced particle size and polydispersibility could be attributed to the stabilization of the colloidal system. Zeta potential and electrophoretic mobility were found to be -3.73 mV and -2.909×10^{-5} $\text{cm}^2/\text{V s}$. The high zeta potential can be said to reduce the tendency for particle aggregation due to higher magnitude of repulsive forces.

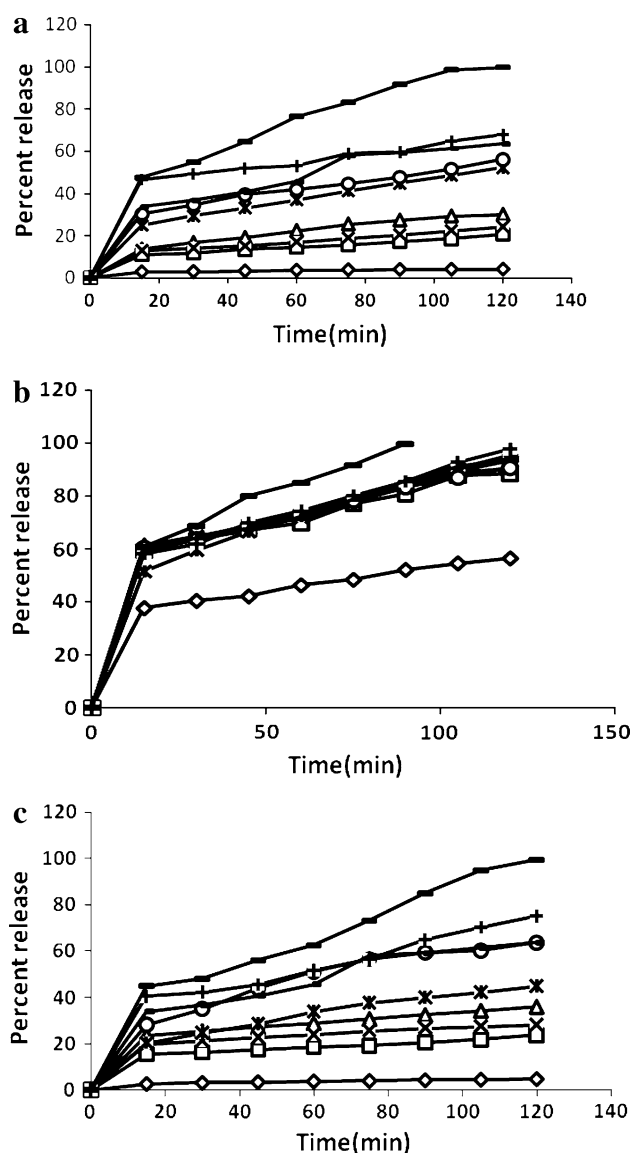


Fig. 11 Dissolution profiles of TEL and complexes of TEL in **a** distilled water, **b** 0.1 N HCl and **c** phosphate buffer pH 6.8
 —◇— TEL —□— IC1 —△— IC2 —×— IC3 —*— IC4 —○— IC5 —+— IC6
 —■— IC7 —●— IC8

Scanning electron microscopy

SEMs of selected preparations were taken which included pure drug TEL, β -CD, NS and drug loaded NS. Characteristic needle shaped crystals of the TEL can be observed in Fig. 10a. As compared to β -CD, NS was porous in nature which was confirmed by surface morphology of β -CD and NS (Fig. 10b, c). A prominent change in the surface morphology was observed in case of solid dispersion with NS (Fig. 10d) i.e. pores of NS partially filled by drug.

In vitro dissolution studies

As compared to plain TEL, inclusion complexes showed faster release. The complex of TEL with NS showed slower release than plain β -CD complex (Fig. 11). In vitro studies revealed slow release of TEL from NS over a period of 2 h. The physical mixtures of TEL with the various NSs showed a negligible change in dissolution. The binary complexes with all the NSs prepared using different ratios of NS and DPC were found to enhance the solubility as well as control the release rate of drug in water (Fig. 11a). Binary complex IC2 (NS:DPC–1:4) showed comparatively higher release than IC1 (NS:DPC–1:2) and IC3 (NS:DPC–1:6). This could be due to non-inclusion complexation seen in IC1 due to insufficient nanochannels or nanopores and in IC3 could be due to inability of TEL to enter into the larger network of channels and pores created. The initial burst effect thus was probably due to dissolution of TEL which is not present in the formulations as inclusion complex, but is adsorbed or encapsulated as non-inclusion complex on the NS surface. After the initial effect, linear and controlled release profiles of the drug was observed. Drug release profiles also depended on the physiological medium. In this case the drug was released faster if the pH was decreased to 1.2, while release was very slow at pH 6.8. This might due to pH dependent solubility of TEL. Over a period of 2 h, 88–95 % drug was released in 0.1 N HCl for all the binary complexes (Fig. 11b). Binary complex with β -CD (IC4) showed a release of 52 % in D.W, 90 % in 0.1 N HCl and ~45 % in pH 6.8 in 2 h (Fig. 10c). Drug release was higher in case of ternary complex of TEL with NS2 and NaHCO_3 (IC6) i.e. 67.68 % in distilled water, 75.05 % in phosphate buffer pH 6.8 and 97.67 % in 0.1 N HCl. Ternary complex with β -CD (IC8) exhibited a significantly higher release of 99 % in 100 min. We can infer from this that supramolecular complexes of guest molecule (TEL) are formed within the intricate network of nanochannels present in NSs. However the release of the drug would also be relatively slow as compared to that from β -CD complexes. The molecular size and conformation may also play an important role as larger molecules with unfavourable stereochemistry may not be easily entrapped within the channels.

In vivo studies

The ternary complexes of TEL with β -CD and with NS i.e. IC6 and IC8, were subjected to in vivo studies since maximum increase in saturation solubility of TEL was evident in all media that were investigated. The pharmacokinetic data shows improved bioavailability of ternary complexes of TEL with NS and β -CD as compared to pure

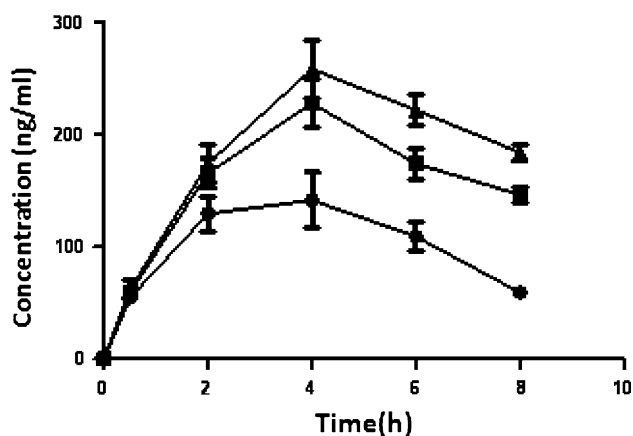


Fig. 12 Plasma concentration time profile of TEL in rats
 ● TEL, ◆ IC6, ▼ IC8

Table 6 Pharmacokinetic parameters of TEL inclusion complexes

Pharmacokinetic parameter	TEL	IC6	IC8
AUC _{0–8 h}	840.86 ± 6.51	1298.43 ± 8.96	1510.61 ± 10.57
C _{max} (ng/ml)	141.32 ± 5.29	227.62 ± 9.54	258.12 ± 8.91
t _{max} (h)	4	4	4

drug (Fig. 12). An increase of 54.4 % in AUC was seen in case the ternary NS complex whereas β -CD ternary complex exhibited an increase of 79.65 % (Table 6). The C_{max} was also found to be enhanced from 141 ng/ml for plain TEL to 227 and 258 ng/ml for IC6 and IC8, respectively. The relatively higher AUC_{0–8 h} displayed by the ternary complex with β -CD and NS corroborates in vitro findings that both β -CD and NSs have the ability to form supra-molecular complexes with TEL. However the release of TEL from NS cavities could be slower than that from β -CD, thereby accounting for the higher AUC and C_{max} seen in case of ternary complexes with β -CD. The nanocavities within the NS structure facilitate entrapment of the drug molecule as well as permit a controlled release under in vivo conditions. Presence of NaHCO₃ helps to modulate pH_M thereby having a positive impact on the solubility of TEL.

Conclusion

The present study involved preparation of drug loaded NS of TEL by incorporating NaHCO₃ using solvent evaporation method. The NSs were found to have spherical shape and colloidal size. CD-based NS was able to complex efficiently with TEL. Solubility studies showed a significant and linear increase in the aqueous solubility with increasing concentration of NS. Ternary complexes of TEL

with β -CD and NSs exhibited highest solubility and in vitro drug release with the NS complex showing a more controlled release profile. Improvement in bioavailability was observed from same inclusion complexes. Thus NSs have the ability to not only increase the intrinsic solubility of TEL but also to provide a controlled release which can be further modulated by including various excipients to form ternary systems.

Conflicts of interest The author reports no conflicts of interest financial or otherwise.

References

- Rossi, S., Ferrari, F., Bonferoni, M.C., Caramella, C.: Characterization of chitosan hydrochloride–mucin interaction by means of viscosimetric and turbidimetric measurements. *Eur. J. Pharm. Sci.* **10**, 251–257 (2000)
- Rekharsky, M.V., Inoue, Y.: Complexation thermodynamics of cyclodextrins. *Chem. Rev.* **98**, 1875–1918 (1998)
- Connors, K.A.: The stability of cyclodextrin complexes in solution. *Chem. Rev.* **97**, 1325–1358 (1997)
- Szejtli, J.: Introduction and general overview of cyclodextrin chemistry. *Chem. Rev.* **98**, 1743–1754 (1998)
- Cavalli, R., Trotta, F., Tumiatti, W.: Cyclodextrin-based nanosponges for drug delivery. *J. Incl. Phenom. Macrocycl. Chem.* **56**, 209–213 (2006)
- Swaminathan, S., Pastero, L., Serpe, L., Trotta, F., Vavia, P., Aquilano, D., Trotta, M., Zara, G., Cavalli, R.: Cyclodextrin-based nanosponges encapsulating camptothecin: physicochemical characterization, stability and cytotoxicity. *Eur. J. Pharm. Biopharm.* **74**, 193–201 (2010)
- Velasquez, M.T.: Angiotensin II receptor blockers, a new class of antihypertensive drugs. *Arch. Fam. Med.* **5**, 351–356 (1996)
- Nakatani, M., Takeshi, S., Ohki, T., Toyoshima, K.: Solid TEL pharmaceutical formulations. US Patent 2004/0110813 A1, 2004
- Phuong, H.L.T., Huyen, T.T., Beom-Jin, L.: Modulation of microenvironmental pH and crystallinity of ionizable TEL using alkalizers in solid dispersions for controlled release. *J. Control. Release* **129**, 59–65 (2008)
- Trotta, F., Tumiatti, W.: Cyclodextrin-based NS as a vehicle for antitumoral drugs. World Patent Number WO/2009/003656, 2009
- Higuchi, T., Connors, K.: Phase solubility techniques. In: Reilly, C. (ed.) *Advances in Analytical Chemistry and Instrumentation*, pp. 117–212. Wiley–Interscience, New York (1965)
- Swaminathan, S., Vavia, P.R., Trotta, F., Torne, S.: Formulation of betacyclodextrin based nanosponges of itraconazole. *J. Incl. Phenom. Macrocycl. Chem.* **57**, 89–94 (2007)
- Marques, M.: Dissolution media simulating fasted and fed state. *Dissolution Technol.* **11**(2), 16 (2004)
- Shimasaki, M., Yamashit, K.: Pharmacokinetics of ¹⁴C-TEL (2): plasma concentration and distribution of ¹⁴C-TEL after repeated oral administration to rats. *Xenobiol. Metab. Dispos.* **14**, 432–436 (1999)
- Brahmankar, D.M., Jaiswal, S.B.: *Biopharmaceutics and Pharmacokinetics: A Treatise*. Vallabh Prakashan, New Delhi (2005)
- Chada, R., Kashid, N., Saini, A.: Account of analytical techniques employed for the determination of thermodynamics of inclusion complexation of drugs with cyclodextrins. *J. Sci. Ind. Res.* **63**, 211–229 (2004)